American Journal of Condensed Matter Physics 2017, 7(2): 50-56
DOI: 10.5923/j.ajcmp.20170702.03

Contribution to the Understanding of III-V Based Nanohole Filling

Antal Ürmös*, Zoltán Farkas, Ákos Nemcsics

Institute of Microelectronics and Technology, Óbuda University, Budapest, Hungary

Abstract A model of filling dynamics of nanoholes will be detailed in this paper. The filling material will be modelled as a viscous liquid. The structure of this paper is as follows. The forming of nanoholes will be briefly described and the filling of these nanoholes will be detailed with and without surface diffusion. The modelling algorithm will be shown for InAs / InGaAs substrate. The description of the modelling algorithm, one possible microscopic interpretation of the viscosity will studied as well. In addition, the number of layers and the equilibrium height relation will be investigated at different temperatures. Furthermore both the viscosity and equilibrium height will be investigated as the function of the temperature. Out investigations will be carried out at macroscopical and microscopical levels as well.

Keywords Nanohole-filling, Droplet epitaxy, GaAs, Modelling, Simulation

1. Introduction

The number of utilization of nanostructures grows permanently. Examples for this the production process of LEDs [1], lasers [2] and GaAs based solar cells [3]. The construction of these GaAs based devices depends to a large extent on fabricating both semiconductor crystal layers and nanostructures. The fabrication process is carried out primarily with molecular beam epitaxy (hereinafter MBE) [4, 5]. Different structures are produced by different methods. A widely used method for the growth of quantum dots is the Stransky-Krastanov method. A relatively new method is the droplet epitaxy which is based on the Volmer Weber method. The principle of droplet epitaxy was invented by Koguchi et al. at the beginning of 1990's. The first step of this process is a deposition of a III main group (eg. In or Ga) droplet onto the substrate (eg. GaAs or AlGaAs). During the second step, the droplets crystallizes and nanostructures are formed. The type of nanostructure is determined as a function of both the pressure of gas phase of V main group element (eg. arsenic) in the environment of the droplet and the temperature of the substrate. This method is useful to produce quantum rings [10], nanoholes [11] and other nanostructures, in addition to quantum dots. Inverse technology quantum dots can be also produced by filling nano holes [12, 13]. A good review on this subject is [14].

Nano holes are produced by local thermal etching on AlGaAs substrate at temperature of T=550-640°C. It is possible to carry out partial or complete burying in case of nano holes. Elevations of size of some nanometers can be observed above the buried quantum dots [14]. Vertically stacked quantum dot molecule can be produced by sequential filling. This structure contains two closely positioned quantum dots. That is the simplest system of interacting nanostructures. Vertically stacked quantum dots consist of two twice buried quantum dots of ultra-low density. In case of GaAs/InAs substrate the dots are separated by a GaAs barrier of a well-defined width. In case of AlGaAs/GaAs substrate, the separating barrier is of AlGaAs. According to the literature there are experimental results of GaAs inverted quantum dots produced on AlGaAs substrate and InAs and InGaAs inverted quantum dots on GaAs substrate. In this paper the model of filling a nanohole created with In/Ga droplet on GaAs substrate is presented. The filler material is InAs/InGaAs.

2. Details of the Simulation Algorithm

Our model takes into consideration only the movement of metal component because the location of transformation into semiconductor state (crystallization) is not influenced by the non-metallic component according to the experiments [11]. The initial parameters are illustrated on Figure 3. D_{ring} is the width of the ring (the difference between the outer circle radius and inner circle radius). The D_{hole} is the diameter of the hole, L is the height of the ring above the substrate, H is the height of the ring above the bottom of the hole. Parameter α is the half angle of the orifice of the hole. This angle is 55°. The parameters are explained on Figure 1.

* Corresponding author:
urmos.antal@phd.uni-obuda.hu (Antal Ürmös)
Published online at http://journal.sapub.org/ajcmp

In each step, 2 monolayers of Indium were deposited. The layers were stacked onto each other. The atoms migrate on the surface during the growth interrupt. For more information about the filling process, please see the ref. [11]. The In atoms deposited from evaporated gas phase.

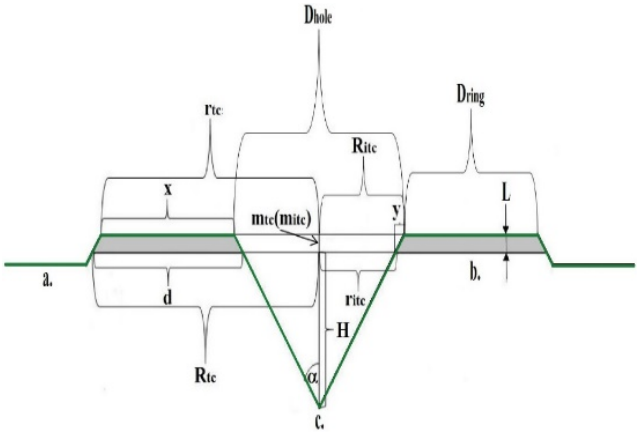

Figure 1. The structure of the investigated nano hole, where (a.) is the area surrounding the nanohole, (b.) ring, around the nanohole and (c.) is the nanohole. The "*itc*" index is the abbreviation of the inner truncated cone

This volume can be calculated as $V_I = r_{hole}^2 * \pi * \delta$ where r_{hole} is the radius of the hole and δ is the thickness of the deposited material.

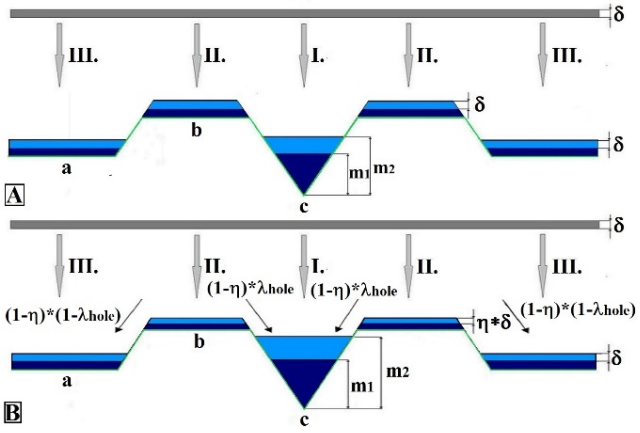

Figure 2. Illustration of volumes deposited onto different parts of the nanohole after depositing two layers. The first deposited layer appears in dark blue, the second deposited layer is light blue. The thickness of the layer on the ring and aside the ring is δ. There is no diffusion in case (A), there is diffusion in the case (B). The arrows illustrate that proportion (1-η) * λ_{hole} (where $\lambda_{hole} = r_{hole} / r_{tc}$) of the volume on the ring gets into the orifice. The λ_{hole} *is the* radius proportional factor of the nanohole, r_{hole} is the radius of the nanohole and r_{tc} is the radius of the entire truncated cone. The (1-η)*(1- λ_{hole}) part gets to the environ of the nanohole. For detailed description, see the next chapter

The volume of the entire truncated cone:

$$V_{tc} = 2.13 * m_{tc}^3 - m_{tc}^2 * (4.48 * d - 6.4 * H) + m_{tc} * (3.14 * d^2 + 8.97 * d * H + 6.4 * H^2), \quad (1)$$

where m_{tc} is the height of the entire truncated cone (it is the same as the thickness of the deposited material), a d is the lower plateau of the ring, the rest of the variables are the same as above. The "*tc*" index is the abbreviation of the truncated cone. As it is mentioned, the half angle of the nanohole is 55°. As a consequence, the value of the constants in this formula 2.13 = 1/3*(π*tg²55), the π*tg55 = 4.48, the π*tg²55 = 6.4, the 2*π*tg55 = 8.97 and the value of π is 3.14.

Advisedly what was discussed so far $V_{II.}$ Volume of the ring can be easily calculated with formula $V_{II} = V_{tc} - V_{itc}$. After simplifying our result, the subsequent formula can be obtained:

$$V_{II.} = -m_{ring}^2 * (4.48 * d + 12.81 * H) + m_{ring} * (3.14 * d^2 + 8.97 * d * H), \quad (2)$$

where m_{ring} is the height of the ring (in this case the thickness of the deposited material), the other variables are the same as above. As a consequence, the value of the constants in this formula π*tg55 = 4.48, the 2*π*tg²55 = 12.81, the 2*π*tg55 = 8.97 and the value of π is 3.14.

3. The Inclusion of Atomic Movement

If one wishes to present a realistic model the atoms move on the surface of the substrate at ($n * k * T > E_{bonding}$) temperature. This movement can be modelled in several ways, eg. a Kinetic Monte-Carlo method [17, 18]. In this paper the temperature dependent dynamic viscosity of liquid Indium will be taken into consideration instead.

In a macroscopic context dynamic viscosity is a proportional factor, which depends on the properties of the liquid. This factor shows the relation between the shear stress and the deformation velocity, which can be calculated by the $\tau=\mu*d\gamma/dt$ formula. In this equation, τ is the shear stress, μ is the dynamical viscosity and the $d\gamma/dt$ is the deformation velocity.

This viscosity can be calculated in different ways for liquid metals [19-23]. In this paper the Arrhenius-Andrande formula will be used [23]:

$$\mu(T) = \mu_0 * e^{\frac{E_0}{R*T}}. \quad (3)$$

where μ(T) is the dynamic viscosity as a function of temperature, T is temperature (on Kelvin scale), the μ_0 is a pre-exponential factor (in case of Indium 0.302), E_0 is the bulk activiation energy (in case of Indium 6650 J/mol), and R is universal gas constant (8,3144 J/(K*mol)).

In nanoscopic approach the probability of occurring of an event must be determined at atomic level dynamic [18, 17]:

$$P(E_a, T) = e^{-\frac{E_a}{R*T}}, \quad (4)$$

where E_a is the activation energy of the event, The k frequency of change of location can be determined with formula $k=k_0*exp(-E_a/(R*T))$ where k_0 is the atomic vibration frequency ($k_0=(2*k_B*T)/h$), where k_B is Boltzmann constant, h is the Planck constant. The next step will be determining the $\rho=\rho(E_a,T)$ geometric factor [24]:

$$\rho(E_a, T) = l * e^{\frac{2E_a}{R*T}}, \quad (5)$$

where l is a scalar. We define E_0 as $E_0=E_a[n]$, where $E_a[n]$ is a density functional which defines the binding energy of the

multeity of n atoms with taking into consideration atom-atom, atom-electron and electron-electron interactions. It follows that the dynamic viscosity can be calculated with formula $\mu(T) = \rho(E_0,T)*k = k_0*l*exp(E_0/(R*T))$, where k_0*l product is the a μ_0 pre-exponential factor. This way equation (4) is obtained.

The effect of viscosity is taken into consideration by multiplying the volume, which is deposited onto the ring with a $\eta(T)$ volume proportionality factor which is calculated as follows: $\eta(T)=\mu(T)/\mu(T_m)$, where $\mu(T)$ is dynamic viscosity as a function of temperature T, and $\mu(T_m)$ is dynamic viscosity as a function of the melting temperature T_m. It follows that the volume V_{II}. that remains on the ring can be calculated with a proportionality factor applied to the total volume that is deposited onto the ring $V'_{II} = \eta*V_{II}$. The thickness of the material that remains on the ring is linearly proportional with viscosity, thus $m_{ring} = \eta*\delta$. It follows that

$$V'_{II.} = -(\eta * \delta)^2 * (4.48 * d + 12.81 * H) + (\eta * \delta) * (3.14 * d^2 + 8.97 * d * H). \quad (6)$$

Similarly to the (2) and (3) equations, the value of the constants in this formula $\pi*tg55 = 4.48$, the $2*\pi*tg^2 55 = 12.81$, the $2*\pi*tg55 = 8.97$ and the value of π is 3.14.

From the formula above it is obtained that the volume that gets into the nanohole is the sum of volume that gets directly into the hole and volume that gets indirectly into the hole $V'_I=V_I+V''_{II}$. This volume can be calculated with formula $V''_{II} = (1-\eta) * \lambda_{hole} * V_{II}$. In the first approach, $\lambda_{hole}=0.5$, so the half of the volume, deposited onto the ring flows into the hole, and the other half flows to the outer environ of the ring.

Similarly to the previous section the first step is to deposit a layer of thickness δ (Figure 2/B). On that figure the arrows indicate that (1-η) * λ_{hole} part of the volume deposited onto the ring gets into nanohole and (1-η) * $\lambda_{environ}$ gets aside the ring ($\lambda_{environ} = 1 - \lambda_{hole}$). The thickness of deposited layer on the ring is $\eta*\delta$, and the thickness of the deposited layer aside the ring is δ. This formula can be generalized the subsequent way:

$$m_i = \sqrt[3]{\frac{3*\sum_{k=1}^{i} V'_{I.k}}{6.4}}, \quad (7)$$

where m_i is the filled up thickness in step, and $\sum_{k=0}^{i} V'_{I.k}$ is the sum of volumes deposited from 1-st step to the *i*-th step. Variable α is the half angle of the orifice of the hole (55°). As a consequence, the value $\pi*tg^2 55 = 6.4$.

4. Evaluation and Discussion

The object of our interest was to examine how the nanohole gets filled with deposited Indium as a function of substrate temperature before the Indium crystallizes. During the filling process the height of the ring that surrounds the nanohole grows as well. In other words, we looked for the phase of In deposition at which the height of material covering the nanohole and the height of the ring are equal. The two heights are considered equal if the respective difference is between zero and one. The average of the two heights is the equilibrium height. During the simulation we sought the temperature at which the height difference of a given deposition layer is minimal.

On Figure 3 the filling process of the nanohole is shown. If the temperature dependence of the viscosity is considered negligible then the height equivalence appears at the 21st layer. The Reader should take into consideration that each deposited layer implies that two monolayers are deposited.

In case of GaAs substrate, the lattice constant is 0.526 nm. That distance equals two monolayers since there are two components. The software code used in the simulation orders 10 pixels to one monolayer that is 0,284/10 = 0,0284 nm per pixel. If a InGaAs inverted dot is placed in GaAs matrix, then there is no misfit in the case of low In concentration and small dot. Distortion appears in the InGaAs lattice. The lattice constant can be used for further calculation. The simulation results was obtained from a simulation software, developed by us in the Microsoft Visual Studio 2015 environment, using the C# language.

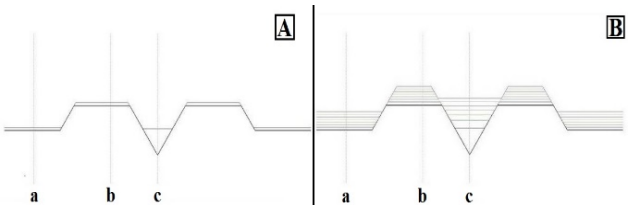

Figure 3. The filling process of the nanohole, in case of 1 **(A)**, 7 **(B)** layers

This ideal case can be observed at substrate temperatures less than 180°C. Above this temperature the equilibrium height and the equilibrium number of layers decreases. As it can be seen on Figure 4 at temperature 188°C the nanohole gets filled completely at the 16th layer where equilibrium height is 13.1. The lower line is the filling height over the orifice of the nanohole (measurement point C), the height of the upper ring is measurement point B. At the intersection point of the two lines is the equilibrium height. On the partial figures the value pairs of equilibrium height and equilibrium number of layers are signed with solid line. As it can be seen to a unit of decrease of equilibrium height belongs increasingly larger change of temperature. Measurement point „ ***a***" was chosen as a reference point.

In the Figure 5. the temperature-equilibrium height (top), and the viscosity-equilibrium height (bottom) diagrams are shown, in the investigated temperature range.

We must first calculate the maximal value of microscopic viscosity in order to get the microscopic temperature viscosity diagram. We start this process with formula (4). The activation energy of indium particles is obtained from formula $E_p = E_0 * (1 - 6*\alpha*r/D)$ [25]. In this formula the E_0 is cohesion energy (also called as bulk activation energy which is 6650 J/mol for Indium), E_p is cohesion energy of metal drops, the α is the form factor (the value of this factor is 1 for spherical particles), r is the radius of an atom, D is the size of the particle. Let the melting temperature of indium droplets

349.42 Kelvin (76,27°C). The size of the particle can be obtained from $D = (9*r*T_{mb}) / (T_{mb} - T_{mp})$ formula [26].

The macroscopic viscosity of Indium was calculated with Arrhenius-Andrande formula (4) [23]. The respective macroscopic temperature-viscosity diagram can be seen on Figure 6.

T_{mb} is the melting point temperature of the bulk material and the T_{mp} is the melting point of the particles of the material. Using this expression, the atomic radius is $1{,}55*10^{-10}$ m and the size of the particle (at 349.42 Kelvin temperature) is $7{,}5688*10^{-9}$ m. Using E_p = 3568 J/mol activation energy and T_{mp} = 349.42 K melting temperature the value of maximal microscopic viscosity is 1.9486 mPa*s.

At nanoscopic level the In temperature viscosity value pairs are shown on Figure 7. A formula of two term power function is fitted to the series of value pairs. The maximal relative error of fitting is 1%.

If a power function of two terms is fitted to this series of dots, the viscosity temperature will be $\mu_{p,Mi}(T) = a*x^b + c$ [27]. The $\mu_{p,Mi}(T)$ is the temperature-viscosity value as a function of the value and a, b, c values are the fitting constants. The value parameter a is $9.089*10^6$, the value of parameter b is -2.566, the value of parameter c is 0.645. The upper diagram is the fitted function, the lower diagram is the absolute error of the fitting. The maximal absolute value is 0,0006311 (the relative error is 0,04%), which occurs at 263.35°C (536.5 °K) temperature.

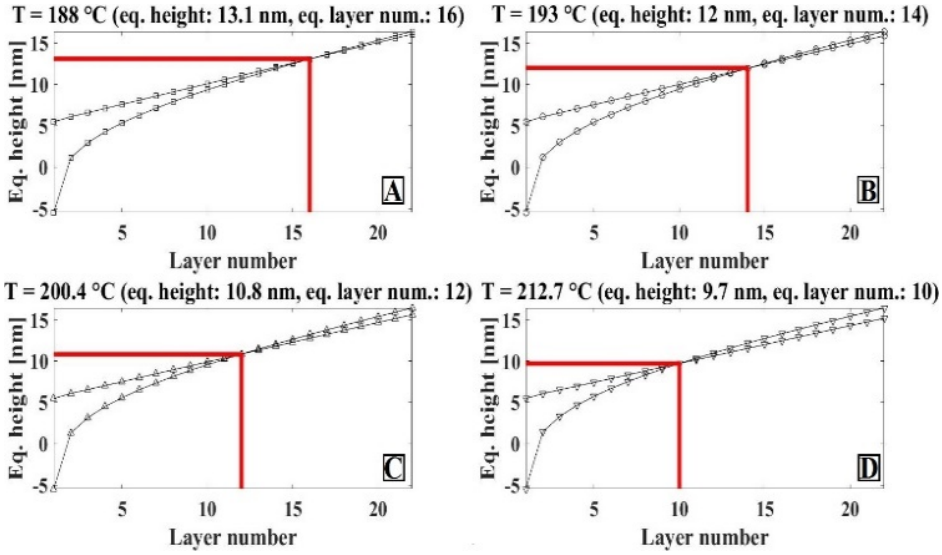

Figure 4. Layer number and equilibrium height diagrams at different temperatures

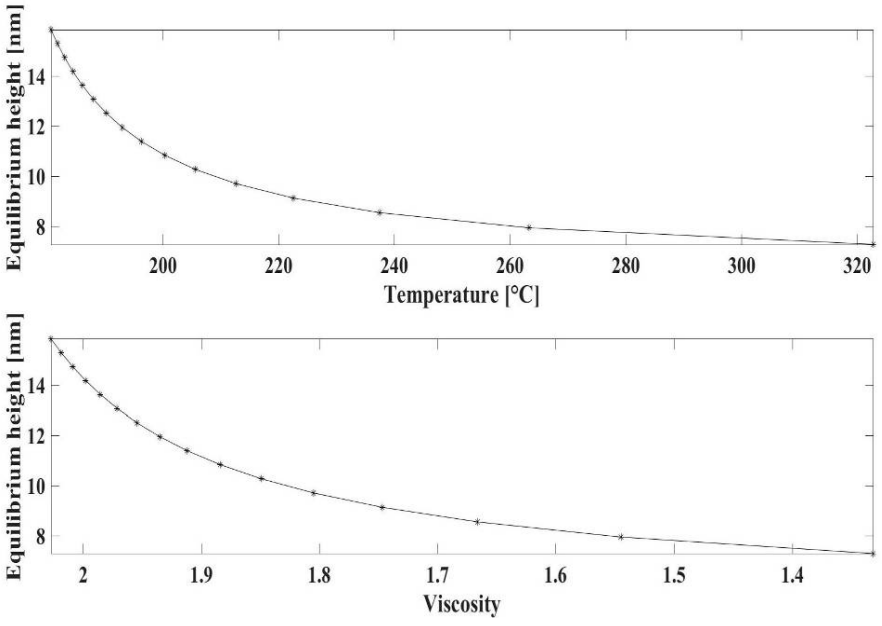

Figure 5. The temperature-equilibrium height (top), and the viscosity-equilibrium height (bottom) diagrams

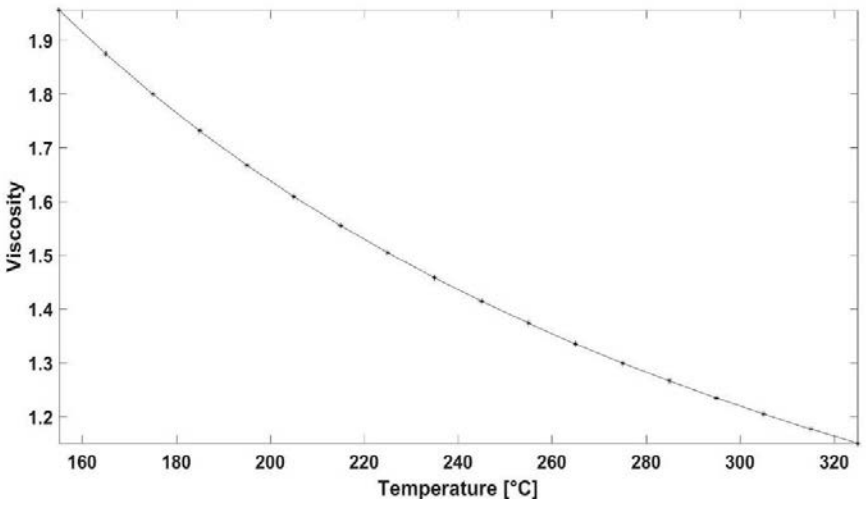

Figure 6. The macroscopic temperature-viscosity diagram of Indium

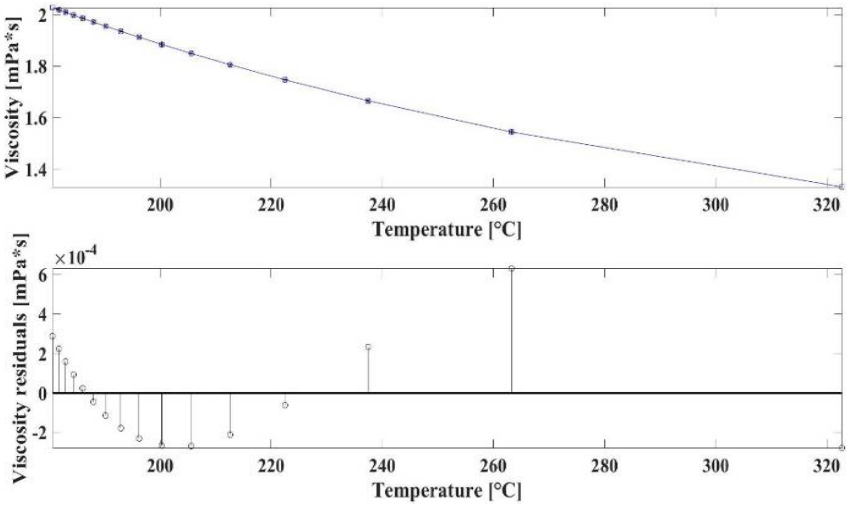

Figure 7. The nanoscopic temperature-viscosity diagram. In this figure, a power-law function is fitted to the point series. In the top part the fitted power-law function and in the bottom part the absolute error of the fitting is shown

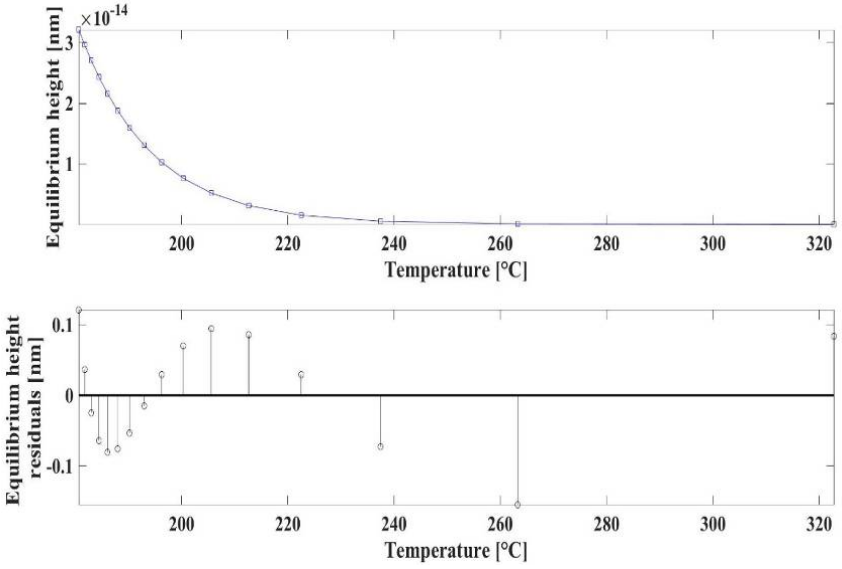

Figure 8. The nanoscopic temperature-viscosity diagram. In this figure, an exponential sum function is fitted to the point series. In the top part the fitted exponential sum function and in the bottom part the absolute error of the fitting is shown

If parameter a is set to $k_0*l = \tau_0$, parameter b is set to 1, parameter c is set to 0 and $x = exp(E_0 / (R*T))$, then expression (4) is obtained again. From this train of thoughts one may conclude that the $\mu_{p,Mi}(T) = a*x^b + c$ formula is the microscopic form of equation (4).

If we fit exponential sum function onto the temperature-equilibrium height value pair sequence in order to analytically determine the equilibrium height (Figure 8.). This way we obtained the formula $h_e(T) = a*e^{bx} + c * e^{dx}$. In the expression the variable $h_e(T)$ is the equilibrium height as a function of temperature, a, b, c, d values are material dependent constants. The values a, b, c, d are $1.398*10^{14}$, -0.06772, 22.77, -0.001933 respectively. Again, the upper diagram is the function fitted to dot sequences, the lower diagram is the absolute error of the fitting at each point. The maximal value of the fitting error is 0.1548 (the relative error is 1.94%), that can be found at 263.35°C (536.5 °K).

5. Conclusions

A possible model of the filling of nanoholes was discussed in this paper. The filler material was modelled as a viscous liquid. During the simulation the behaviour of the In was investigated in heated substrate during the evaporation. First, the case was investigated, when there is not surface diffusion, so there is no atomic displacement on the surface. After this, the atomic displacement was considered, so that the atomic ensemble was regarded as the viscous liquid, the movement of which corresponds to the surface diffusion. Next to the description of the modelling algorithm, one possible microscopical interpretation of the viscosity was studied as well. In addition, the layer number and the equilibrium height relation was investigated at different temperatures. Furthermore, the viscosity was investigated as a function of the temperature and the equilibrium height as a function of the temperature as well. Our research covered both the macroscopic and microscopic level. The equilibriums height depends on the temperature.

REFERENCES

[1] Shuji Nakamura, "Background Story of the Invention of Efficient Blue InGaN Light Emitting Diodes," Aula Magna, Stockholm University, Sweden, 2014.

[2] Mohamed Henini, "Quantum dot nanostructures," *Materials Today*, vol. 5, no. 6, pp. 48-53, 2002.

[3] A. Luque, A. Martí, C. Stanley, "Understanding intermediate-band solar cells," *Nature Photonics*, vol. 6, pp. 146–152, February 2012.

[4] Prof. Dr. M. A. Herman, Dr. H. Sitter, M*olecular Beam Epitaxy, Fundamentals and Current Status 2nd. ed.* Berlin: Springer, 1996.

[5] Mohamed Henini, Ed., *Molecular Beam Epitaxy: From Research to Mass Production.:* Elsevier Science, 2012.

[6] N. Koguchi, S. Takahashi, T. Chikyow, "New MBE growth method for InSb quantum well boxes," *Journal of Crystal Growth*, pp. 688-692, 1991.

[7] N. Koguchi, K. Ishige, "Growth of GaAs Epitaxial Microcrystals on an S-Terminated GaAs Substrate by Successive Irradiation of Ga and As Molecular Beams," *Japanese Journal of Applied Physics*, vol. 32, no. 5A, p. 2052, 1993.

[8] T. Chikyow, N. Koguchi, "MBE Growth Method for Pyramid-Shaped GaAs Micro Crystals on ZnSe(001) Surface Using Ga Droplets," *Japanese Journal of Applied Physics*, vol. 29/2, no. 11, p. 2093, 1990.

[9] S. Sanguinetti, N. Koguchi, "Droplet Epitaxy of Nanostructures," in *Molecular Beam Epitaxy: From Research to Mass Production*, 1st Edition. Waltham, MA, USA: Elsevier Science, 2013, pp. 95-111.

[10] T. Kuroda, T. Mano, T. Ochiai, S. Sanguinetti, K. Sakoda, G. Kido, N. Koguchi, "Optical transitions in quantum ring complexes," *PHYSICAL REVIEW B*, vol. 72, p. 205301, 2005.

[11] C. Heyn, D. Sonnenberg, and W. Hansen, "Local Droplet Etching: Self-assembled Nanoholes for Quantum Dots and Nanopillars," in *Nanodroplets.* New York: Springer Science, 2013, pp. 363-383.

[12] Ch Heyn, T. Bartsch, S. Sanguinetti, D. Jesson, W. Hansen, "Dynamics of mass transport during nanohole drilling by local droplet etching," *Nanoscale Research Letters*, pp. 10-67, Dec. 2015.

[13] Á. Nemcsics, B. Pődör, L. Tóth, J. Balázs, L. Dobos, J. Makai, M. Csutorás, A. Ürmös, "Investigation of MBE grown inverted GaAs quantum dots," *Microelectronics Reliability*, vol. 59, pp. 60-63, 2016.

[14] Á. Nemcsics, Ch. Heyn, L. Tóth, L. Dobos, A. Stemmann, W. Hansen, "Cross-sectional transmission electron microscopy of GaAs quantum dots fabricated by filling of droplet-etched nanoholes," *Journal of Crystal Growth*, vol. 335, no. 1, pp. 58–61, November 2011.

[15] R. Timm, H. Eisele, L. Ivanova, D. Martin, V. Voßebürger, A. Rastelli, O. G. Schmidt, M. Dähne A. Lenz, "Structural investigation of hierarchically self-assembled GaAs/AlGaAs quantum dots," *Phys. Stat. Sol. (b)*, vol. 243, no. 15, pp. 3976–3980, May 2006.

[16] P.G. Eliseev et al., "Ground-state emission and gain in ultralow-threshold InAs-InGaAs quantum-dot lasers," *IEEE JOURNAL ON SELECTED TOPICS IN QUANTUM ELECTRONICS*, vol. 7, no. 2, pp. 135-142, 2001.

[17] L. Nurminen, A. Kuronen, K. Kaski, "Kinetic Monte Carlo simulation of nucleation on patterned substrates," *Phys. Rev. B*, vol. 63, no. 3, p. 035407, December 2000.

[18] W. Miller, "Simulation of Epitaxial Growth by Means of Density Functional Theory, Kinetic Monte Carlo, and Phase Field Methods," in *Handbook of Crystal Growth: Fundamentals (Volume I., Part A: Thermodynamics and Kinetics)*, 2nd ed. New York: Elsevier B.V, 2015, pp. 521-559.

[19] L. Battezzati, A.L. Greer, "The viscosity of liquid metals and

alloys," *Acta Metallurgica,* vol. 37, no. 7, pp. 1791-1802, 1989.

[20] Seeton, C. J., "Viscosity–temperature correlation for liquids," *Tribology Letters,* vol. 22, no. 1, pp. 67-78, 2006.

[21] K. E. Spells, "The determination of the viscosity of liquid gallium over an extended nrange of temperature,", vol. 48, Proc. Phys. Soc, 1936, pp. 299-311.

[22] M. J. Assael, I. J. Armyra, J. Brillo, S. V. Stankus, J. Wu, W. A. Wakeham, "Reference Data for the Density and Viscosity of Liquid Cadmium, Cobalt, Gallium, Indium, Mercury, Silicon, Thallium, and Zinc," *J. Phys. Chem. Ref. Data,* vol. 41, no. 3, pp. 033101-1-17, 2012.

[23] W.F. Gale, T.C. Totemeier, "General physical properties," in *Smithells Metals Reference Book (Eighth Edition).:* Elsevier Inc., 2004, pp. 1-45.

[24] L. C. Yang, "Frequency Factor in Arrhenius Decomposition Kinetics for Insensitive Energetic Materials," in *American Institute of Aeronautics and Astronautics Inc.,* 45th AIAA/ASME/SAE/ASEE Joint Propulsion Conference & Exhibit, 2009, pp. 1-28.

[25] W.H. Qi, M.P. Wang, "Size and shape dependent melting temperature of metallic nanoparticles," *Materials Chemistry and Physics,* vol. 88, no. 2-3, pp. 280-284, 2004.

[26] D. Xie, M.P. Wang, W.H. Qia, L.F. Cao, "Thermal stability of indium nanocrystals: A theoretical study," *Materials Chemistry and Physics,* vol. 96, no. 2-3, pp. 418-421, 2006.

[27] I.N. Bronshtein, K. A. Semendyayev, G. Musiol, H. Mühlig, "Arithmetic," in *Handbook of Mathematics.* Berlin Heidelberg: Springer, 2007, p. 8.